

High brain lactate is a hallmark of aging and caused by a shift in the lactate dehydrogenase A/B ratio

Jaime M. Ross^{a,b,1}, Johanna Öberg^c, Stefan Brené^d, Giuseppe Coppotelli^e, Mügen Terzioglu^f, Karin Pernold^a, Michel Goiny^g, Rouslan Sitnikov^h, Jan Kehr^g, Aleksandra Trifunovicⁱ, Nils-Göran Larsson^{f,j}, Barry J. Hoffer^b, and Lars Olson^{a,1}

^aDepartment of Neuroscience, Karolinska Institutet, SE-171 77 Stockholm, Sweden; ^bNational Institute on Drug Abuse, National Institutes of Health, Baltimore, MD 21224; ^cDivision of Radiology, Department of Clinical Science, Intervention, and Technology, Karolinska Institutet, SE-141 86 Stockholm, Sweden; ^dDepartment of Neurobiology, Health Sciences, and Society, Experimental Magnetic Resonance Center, Karolinska Institutet, SE-171 77 Stockholm, Sweden; ^eDepartment of Cell and Molecular Biology, Karolinska Institutet, SE-171 77 Stockholm, Sweden; ^fMax Planck Institute for Biology of Ageing, D-50931 Cologne, Germany; ^gDepartment of Physiology and Pharmacology, Karolinska Institutet, SE-171 77 Stockholm, Sweden; ^hInstitute of Neurology, University College London, London WC1N 1PJ, United Kingdom; ⁱCologne Excellence Cluster on Cellular Stress Responses in Aging-Associated Diseases (CECAD), University of Cologne, D-50674 Cologne, Germany; and ^jDepartment of Laboratory Medicine, Karolinska Institutet, SE-141 86 Stockholm, Sweden

Edited* by Floyd Bloom, The Scripps Research Institute, La Jolla, CA, and approved September 20, 2010 (received for review June 14, 2010)

At present, there are few means to track symptomatic stages of CNS aging. Thus, although metabolic changes are implicated in mtDNA mutation-driven aging, the manifestations remain unclear. Here, we used normally aging and prematurely aging mtDNA mutator mice to establish a molecular link between mitochondrial dysfunction and abnormal metabolism in the aging process. Using proton magnetic resonance spectroscopy and HPLC, we found that brain lactate levels were increased twofold in both normally and prematurely aging mice during aging. To correlate the striking increase in lactate with tissue pathology, we investigated the respiratory chain enzymes and detected mitochondrial failure in key brain areas from both normally and prematurely aging mice. We used *in situ* hybridization to show that increased brain lactate levels were caused by a shift in transcriptional activities of the lactate dehydrogenases to promote pyruvate to lactate conversion. Separation of the five tetrameric lactate dehydrogenase (LDH) isoenzymes revealed an increase of those dominated by the *Ldh-A* product and a decrease of those rich in the *Ldh-B* product, which, in turn, increases pyruvate to lactate conversion. Spectrophotometric assays measuring LDH activity from the pyruvate and lactate sides of the reaction showed a higher pyruvate → lactate activity in the brain. We argue for the use of lactate proton magnetic resonance spectroscopy as a noninvasive strategy for monitoring this hallmark of the aging process. The mtDNA mutator mouse allows us to conclude that the increased LDH-A/LDH-B ratio causes high brain lactate levels, which, in turn, are predictive of aging phenotypes.

mtDNA mutator mouse | proton magnetic resonance spectroscopy | *in situ* hybridization | COX/SDH enzyme histochemistry | HPLC

Mitochondrial dysfunction may underlie aging-related alterations (1) in neuronal function and has been implicated in Alzheimer's and Parkinson's disease as well as stroke. The mitochondrial theory of aging (2) suggests damage to mtDNA slowly accumulates with time and causes aging by interfering with bioenergetic homeostasis and/or by loss of cells because of apoptosis and/or replicative senescence (3). High levels of certain mtDNA mutations impair respiratory chain function and cause a plethora of human diseases (4). Normal aging in humans (5, 6), monkeys (7), and rodents (8, 9) is associated with accumulation of mtDNA point mutations and deletions. However, the role of such mutations in aging has been questioned, because the overall level of mtDNA mutations is usually lower than the threshold needed to cause respiratory chain dysfunction (10).

To address the mitochondrial theory of aging experimentally, knock-in mice (mtDNA mutator mice) expressing a proofreading-deficient version of the nucleus-encoded catalytic subunit (PolgA) of mtDNA polymerase were created (11–13). Homozygous knock-in mice have reduced life span and premature onset of human-like aging phenotypes (Fig. S1A), including reduced

fertility, weight loss, reduced s.c. fat, enlarged heart, anemia, alopecia, kyphosis, osteoporosis, sarcopenia, and hearing loss (11–13). A premature aging phenotype has been confirmed in mice generated elsewhere using the same strategy (14). The mtDNA mutator mouse has high levels of mtDNA point mutations (20–30 mutations per mtDNA molecule) as well as increased levels of linear deletions (~25% of total mtDNA) (12, 13); however, the extent of point mutations and/or deletions and their role in aging phenotypes have recently been under debate (15–17). Interestingly, premature aging phenotypes in mtDNA mutator mice seem not to be caused by increased levels of reactive oxygen species (12, 14) but rather, are explained by a decline in oxidative capacity (15). However, the downstream effects of declined cellular respiration on the aging process remain unclear.

Here, we investigated the role of mitochondrial dysfunction and abnormal metabolism on CNS aging using both normally aging mice and prematurely aging mtDNA mutator mice. We found that mitochondrial dysfunction in the brain leads to a metabolic shift from aerobic respiration to glycolytic metabolism, resulting in expression changes of the lactate dehydrogenase genes (LDH-A and LDH-B). This shift results in robustly increased brain lactate levels, detectable using proton magnetic resonance spectroscopy (¹H-MRS), before the appearance of overt aging phenotypes. Our results suggest a unique role for increased lactate as a marker, possibly even presymptomatic, in aging. ¹H-MRS constitutes a noninvasive strategy for monitoring this hallmark of brain aging.

Results

Elevated Lactate Revealed in Brain and Peripheral Tissues. We investigated the mtDNA mutator mouse early in life and in advance of overt aging phenotypes. They displayed a marked increase of the lactate doublet peak at 1.33 ppm in cerebral cortex and striatum, as measured by ¹H-MRS when lactate concentrations were estimated as ratios to total creatine concentration (Cr + PCr) (Fig. 1A–C and Fig. S2A–C). In cerebral cortex (Fig. 1C), lactate levels were increased twofold in 6- to 9-wk-old and threefold in 35- to 38-wk-old mtDNA mutator mice compared with wild-type littermates. The rate of increase of lactate in cerebral cortex from 6–9 to 35–38 wk of age was 2.1%/wk in mtDNA mutator mice (Fig. S2C). In striatum (Fig. 1C), lactate levels were also twofold higher in 6- to 9-wk-old mtDNA mutator mice, and

Author contributions: J.M.R., S.B., G.C., B.J.H., and L.O. designed research; J.M.R., J.Ö., S.B., G.C., M.T., K.P., M.G., R.S., and J.K. performed research; J.Ö., S.B., M.T., R.S., J.K., A.T., and N.-G.L. contributed new reagents/analytic tools; J.M.R., J.Ö., G.C., M.G., and J.K. analyzed data; and J.M.R., B.J.H., and L.O. wrote the paper.

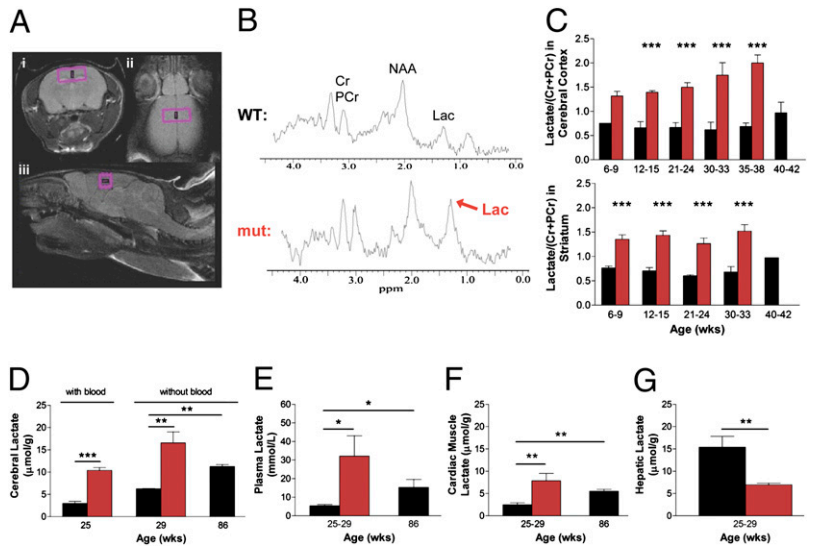
The authors declare no conflict of interest.

*This Direct Submission article had a prearranged editor.

¹To whom correspondence may be addressed. E-mail: rossja@nida.nih.gov or Lars.Olson@ki.se.

This article contains supporting information online at www.pnas.org/lookup/suppl/doi:10.1073/pnas.1008189107/-DCSupplemental.

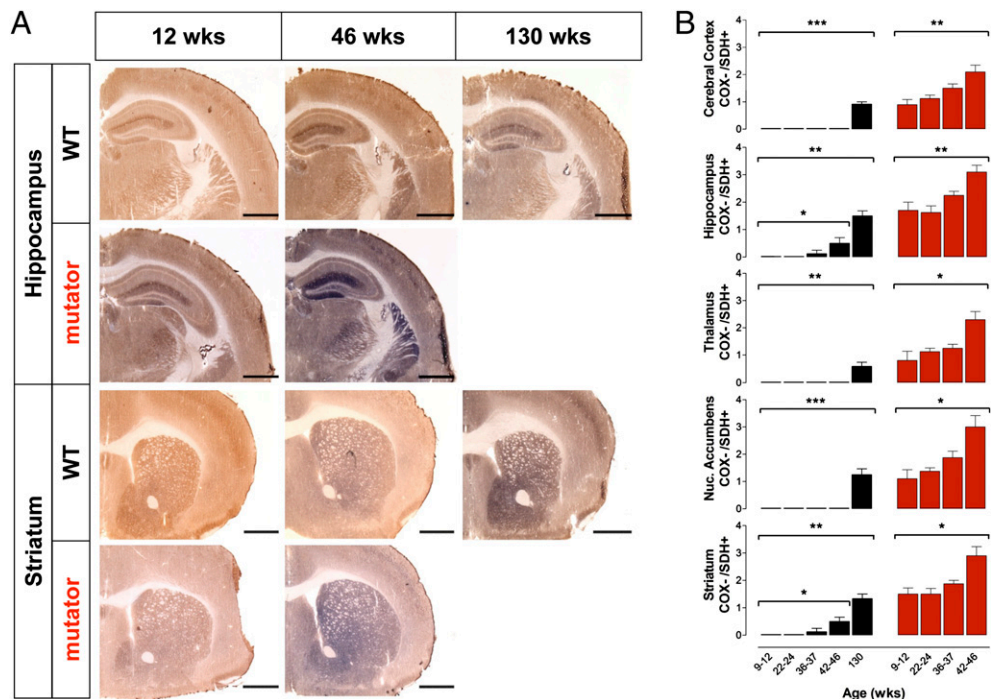
Fig. 1. High lactate levels in brain and peripheral tissues. (A) Position of the volume of interest (VOI) in cerebral cortex in (i) axial, (ii) coronal, and (iii) sagittal planes. (B) Typical $^1\text{H-MR}$ spectra obtained from a VOI in cerebral cortex indicating the marked increase in the lactate doublet (centered on 1.33 ppm) in mtDNA mutator mice. (C) Two-way between-subjects ANOVA on age-matched groups was performed on brain lactate concentrations (mean values \pm SEM) in cerebral cortex (Upper) and striatum (Lower) from female mtDNA mutator ($n = 19$; red) compared with littermate wild-type ($n = 18$; black) mice. All mutator mice showed a significant increase in lactate levels, and ANOVA showed a significant effect for the mtDNA mutator allele both in cerebral cortex [$F(1,25) = 84.1$; $P < 0.0001$] and striatum [$F(1,24) = 134$; $P < 0.0001$] compared with controls. Posthoc analyses are denoted with $***P < 0.001$. (D–G) Analyses of tissue lactate (mean values \pm SEM) measured by HPLC from female 25- to 29-wk-old mtDNA mutator ($n = 6$; red), 25- to 29-wk-old ($n = 6$; black), and 86-wk-old littermate wild-type ($n = 3$; black) mice. (D) The 25- to 29-wk-old mtDNA mutator mice showed a threefold increase in brain lactate with [t(4) = 9.60; $P = 0.0007$] and without [t(4) = 4.20; $P = 0.007$] the presence of blood compared with controls. A twofold increase in brain lactate in 86-wk-old wild-type controls compared with 25- to 29-wk-old controls [t(4) = 16.9; $P = 0.007$] was revealed. (E) Plasma lactate increased sixfold in mtDNA mutator mice compared with 25- to 29-wk-old controls [t(9) = 2.71; $P = 0.024$]. In wild-type mice, plasma lactate levels tripled at 86 wk of age compared with 25- to 29-wk-old animals [t(7) = 3.41; $P = 0.011$]. (F and G) Lactate levels in cardiac muscle were also tripled in mtDNA mutator mice [t(6) = 3.15; $P = 0.009$], whereas levels in hepatic tissue were halved [t(6) = 3.43; $P = 0.007$], both compared with 25- to 29-wk-old controls. Cardiac muscle lactate levels were also increased twofold in 86-wk-old wild-type mice [t(5) = 4.90; $P = 0.002$] compared with 25- to 29-wk-old controls. HPLC significances were determined by two-tailed unpaired t test analysis and denoted with $*P < 0.05$, $**P < 0.01$, and $***P < 0.001$.



these levels were maintained as mtDNA mutator mice aged (Fig. S2C). During normal aging, we found that lactate levels determined by $^1\text{H-MRS}$ increased later in life; between 20 and 42 wk of age, this increase averaged 1.6%/wk in cerebral cortex and 1.7%/wk in striatum (Fig. S3). There have been few $^1\text{H-MRS}$ studies of lactate in animal models of neurodegenerative diseases, possibly because of diffi-

culties in distinguishing the lactate signal from that of overlapping lipids and lipid-type macromolecules (18). To address this potential confounding factor, we used both a short (15 ms) and a long (135 ms) echo time (TE) to minimize potential contamination errors (Fig. S2E). With the long TE, the characteristic phase inversion of the doublet peak to below baseline occurred and revealed an increase in lactate, similar to that seen

Fig. 2. Mitochondrial dysfunction in aging. (A) COX/succinate dehydrogenase (SDH) double labeling to visualize respiratory chain deficiencies, indicated by blue staining, in brains of 9- to 46-wk-old male and female mtDNA mutator ($n = 24$; red) and 9- to 130-wk-old littermate wild-type ($n = 30$; black) mice. (Scale bar: 1.00 mm.) (B) Semiquantification (mean values \pm SEM) of COX deficiency on a scale of 0–4 (0, no blue staining; 4, only blue staining; recorded blindly) shows that mitochondrial respiratory chain dysfunction begins at 9–12 wk in mtDNA mutator mice and becomes widespread in cerebral cortex [$H(4) = 11.7$; $P = 0.008$], hippocampus [$H(4) = 11.8$; $P = 0.008$], nucleus accumbens [$H(4) = 9.59$; $P = 0.022$], striatum [$H(4) = 10.4$; $P = 0.016$], and thalamus [$H(4) = 9.87$; $P = 0.019$] as these mice age. In wild-type mice, there was increased COX deficiency in similar brain regions, indicating respiratory chain dysfunction in normal aging: cerebral cortex [$H(5) = 21.7$; $P = 0.0002$], hippocampus [$H(5) = 18.4$; $P = 0.001$], nucleus accumbens [$H(5) = 21.4$; $P = 0.0003$], striatum [$H(5) = 18.3$; $P = 0.001$], and thalamus [$H(5) = 17.1$; $P = 0.019$]. In wild-type mice, there was also increased COX deficiency in hippocampus [$H(4) = 8.36$; $P = 0.039$] and striatum [$H(4) = 9.10$; $P = 0.028$] over time from the 9- to 12-wk group to the 42- to 46-wk group. Observations were made at all time points, and short lines indicate 0 ratings (no blue staining). Significances from nonparametric data were determined by one-way Kruskal–Wallis ANOVA denoted with $*P < 0.05$, $**P < 0.01$, and $***P < 0.001$.



with the short TE. This suggests that the amount of lactate in mutator mice is sufficient to enable LCModel to resolve lactate confidently from overlapping lipid and lipid-type macromolecules. To exclude the possibility that the genetic background of mutator mice could contribute to the high cerebral lactate levels, we also performed $^1\text{H-MRS}$ in 129/SvImJ and C57BL/6J mice and found them to be similar to our mtDNA littermate control mice (Fig. S2D).

We next measured brain lactate levels in both prematurely and normally aging mice using HPLC to confirm the $^1\text{H-MRS}$ findings and establish that high brain lactate is a marker of normal aging. HPLC showed a threefold increase in brain lactate in 25-wk-old mtDNA mutator mice (Fig. 1D), confirming the $^1\text{H-MRS}$ finding. The increased mtDNA mutator brain lactate levels are pathological compared with age-matched wild-type mice but importantly, are within the range of levels that can be seen under other pathological circumstances, such as stroke (19). Furthermore, brain lactate measurements in wild-type mice are within the physiological range as reported by others (20). Additionally, plasma lactate (Fig. 1E) increased sixfold in mtDNA mutator mice. Therefore, to ensure that lactate was increased in brain tissue per se rather than in blood in the tissue, we perfused additional animals with saline to remove blood (Fig. 1D) and found that lactate remained increased in mtDNA mutator brains. We used this same perfusion strategy to investigate whether high brain lactate also is a marker of normal aging and found a twofold increase in lactate levels in blood-free brains from 86-wk-old wild-type controls. Additionally, plasma lactate (Fig. 1E) increased threefold in these same animals. Thus, brain and plasma lactate levels increased also during normal aging, albeit much later in life.

HPLC showed that cardiac muscle lactate levels increased threefold in 25- to 29-wk-old mtDNA mutator mice and twofold in 86-wk-old wild-type mice (Fig. 1F). Interestingly, hepatic lactate was decreased 2.2-fold in mtDNA mutator mice (Fig. 1G). These data suggest that the high lactate levels in brain, plasma, and heart are caused by dysfunction of the mitochondrial respiratory chain. Cells with dysfunctional mitochondria are less

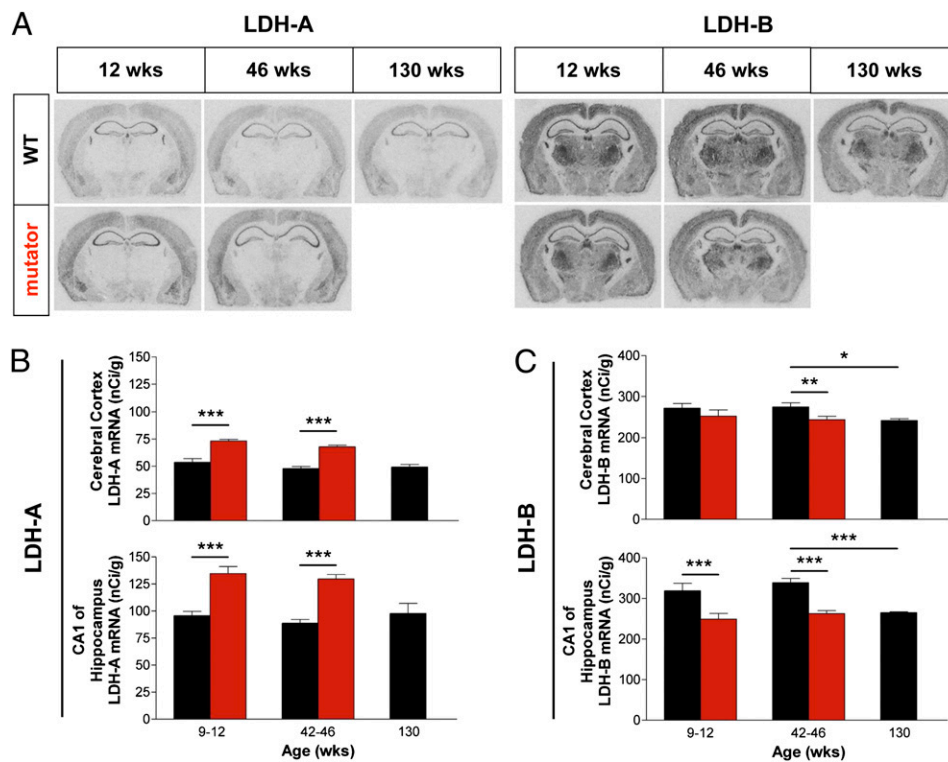
able to metabolize pyruvate through the tricarboxylic acid (TCA) cycle and thus, would rely on glycolysis and anaerobic metabolism. The decreased lactate levels in liver might be caused by an increase in gluconeogenesis to supply peripheral tissues with additional glucose (21, 22).

Mitochondrial Dysfunction in mtDNA Mutator and Normally Aged Mice.

To correlate the striking increase in lactate with tissue histopathology, we used COX/succinate dehydrogenase (SDH) enzyme histochemistry (Fig. 2 A and B) and detected early mitochondrial failure in both normally and prematurely aging mice in key brain regions: cortex, hippocampus, accumbens, striatum, and thalamus. SDH, or complex II of the respiratory chain, is entirely encoded by nuclear DNA, whereas COX, or complex IV, has critical components encoded by mtDNA. Impaired mtDNA typically does not affect complex II activity but leads to severe reduction in complex IV activity. Such respiratory chain-deficient cells will appear blue with the double enzyme histochemistry method, whereas normal cells will appear dark brown. In mtDNA mutator mice, COX activity began to decline at 9–12 wk of age, presymptomatic of other aging phenotypes (visual after 24 wk of age). By 46 wk, there was a further decrease in COX activity in all analyzed brain regions, suggesting widespread exacerbation of respiratory chain dysfunction. Importantly, decreased COX activity was also seen in the same brain regions of wild-type mice as they aged to 130 wk (2.5 y). We found an increase in COX deficiency in hippocampus and striatum beginning at 36–37 wk from these same animals in advance of other indices of aging (Fig. 2B). This shows that such mitochondrial dysfunction is a natural phenomenon of aging and consistent with age-dependent COX deficiency in human brain and peripheral tissues (23). We also found regional differences in COX activity, most notably that cerebral cortex was less affected, supporting the notion that this region may be partially protected from accumulation of mtDNA damage (24). Additionally, single SDH enzyme histochemistry revealed an increase in SDH activity in both normally and prematurely aging brains, suggested

Fig. 3. Lactate dehydrogenase gene expression in brain.

(A) In situ hybridization autoradiographic films of LDH-A and LDH-B mRNA in sections from male and female mtDNA mutator ($n = 22$; red) and littermate wild-type ($n = 26$; black) mice shown at ages 12, 46, and 130 (wild-type only) wk. (B and C) Quantification from autoradiographic films of LDH-A and LDH-B mRNA (mean values \pm SEM), expressed as nCi g^{-1} , in cerebral cortex and CA1 of hippocampus from 9- to 12-wk-old and 42- to 46-wk-old mtDNA mutator compared with age-matched wild-type mice and from 130-wk-old (2.5-y-old) wild-type mice. All mtDNA mutator mice showed an up-regulation of LDH-A mRNA expression, and ANOVA showed a significant effect for the mtDNA mutator allele both in cerebral cortex [$F(1,20) = 80.0$; $P < 0.0001$] and CA1 of hippocampus [$F(1,20) = 74.2$; $P < 0.0001$] compared with controls. ANOVA also determined an overall decrease in LDH-B gene expression, caused by the mtDNA mutator allele, both in cerebral cortex [$F(1,20) = 4.8$; $P = 0.040$] and CA1 of hippocampus [$F(1,20) = 31.4$; $P < 0.0001$] compared with controls. LDH-B mRNA levels in 130-wk-old wild-type mice were significantly decreased both in cerebral cortex [$t(10) = 3.06$; $P = 0.012$] and CA1 of hippocampus [$t(10) = 7.06$; $P < 0.0001$] compared with 42- to 46-wk-old wild-type mice, whereas LDH-A mRNA expression remained constant in 130-wk-old mice. Analyses were performed by two-way between subjects ANOVA with posthoc analysis on age-matched groups (9–12 wk and 42–46 wk) and by two-tailed unpaired t test comparing 130-wk-old wild-type with 42- to 46-wk-old wild-type mice. * $P < 0.05$, ** $P < 0.01$, and *** $P < 0.001$.



by Edgar et al. (15) to be caused by increased mitochondrial biogenesis. These findings coupled with other reports (15–17) provide additional evidence for the argument that aging, particularly mtDNA mutation-driven aging, might be primarily driven by increased levels of mtDNA point mutations rather than mtDNA deletions (15).

Increased LDH-A/LDH-B Gene Expression Ratio. Mitochondrial dysfunction can alter expression of nuclear genes involved in nuclear-mitochondrial cross-talk (25), although the trigger for such signaling is unknown. Cells forced to rely heavily on glycolysis must replenish NAD⁺, which is also accomplished by increasing pyruvate (P) to lactate (L) conversion by lactate dehydrogenase (LDH; EC 1.1.1.27). *Ldh-A* is associated with P → L conversion, and *Ldh-B* with L → P conversion. Using in situ hybridization to map and quantify transcriptional activity (26), we show that increased lactate levels are caused by up-regulation of *Ldh-A* and down-regulation of *Ldh-B*, which promote P → L conversion. The transcriptional activity patterns of *Ldh-A* and *Ldh-B* in wild-type control mice resemble those previously reported (27). Thus, LDH-B mRNA was highly expressed throughout the brain, whereas LDH-A was less widely expressed but with markedly higher levels in cerebral cortex and hippocampus than in subcortical regions (Fig. 3A). LDH-A mRNA levels (Fig. 3A and B) in mtDNA mutator cortex were increased by 36% in 9- to 12-wk-old and 42% in 42- to 46-wk-old mtDNA mutator animals. In hippocampal CA1, LDH-A mRNA levels were increased by 41% in 9- to 12-wk-old and 48% in 41- to 46-wk-old mtDNA mutator mice. In contrast, LDH-B mRNA expression (Fig. 3A and C) in cortex dropped 11% below basal levels in 42- to 46-wk-old mutator mice. In CA1, *Ldh-B* expression similarly fell 22% in both 9- to 12-wk-old and 42- to 46-wk-old age groups. Similarly, LDH-B mRNA levels decreased in 130-wk-old (2.5 y) wild-type controls (by 11% in cortex and 22% in CA1, thus reaching levels typical of 42- to 46-wk-old mutator mice). Our data suggest that the LDH-A/LDH-B gene expression ratio increases in both prematurely and normally aging mice, albeit later in life in the latter, suggesting that the ability to convert P → L in response to decreased aerobic cellular respiration capabilities is a characteristic of aging.

The LDH-A/LDH-B gene expression ratio is also altered in other metabolically active organs (i.e., heart and liver), presumably in response to impaired oxidative phosphorylation (Fig. 4A and B). However, we found that the brain responds differently than heart and liver. In mtDNA mutator heart, where lactate levels are also elevated, *Ldh-B* is down-regulated like in brain, whereas the up-regulation of *Ldh-A* transcription is not nearly as marked as in the brain. In liver from mtDNA mutator mice, the up-regulation of *Ldh-A* exceeds that in brain at all time-points, particularly at 45 wk, with an almost twofold increase. The most marked difference, however, is the threefold concomitant up-regulation of *Ldh-B* in mtDNA mutator liver, which is in stark contrast to the down-regulation of this gene in brain areas. This finding might explain the 2.2-fold decrease in hepatic lactate levels (Fig. 1G). Additionally, we found that the LDH-A/LDH-B gene expression ratio is altered relatively early (between 23 and 45 wk) in wild-type controls from the same peripheral tissues, with increased *Ldh-A* in cardiac muscle and increased *Ldh-B* in hepatic tissue (Fig. 4B). Thus, brain, heart, and liver handle mitochondrial failure differently, depending on local energetic needs and energy reservoirs.

LDH Isoenzyme Composition Shifts Drive Lactate Formation. LDH-A and LDH-B gene products, known as M and H, respectively, combine to form five isoenzymes (Fig. 5A): LDH-1 (H₄), LDH-2 (H₃M₁), LDH-3 (H₂M₂), LDH-4 (H₁M₃), and LDH-5 (M₄) (28), which differ in electrophoretic mobility, K_m lactate, and K_m pyruvate (28). The tissue expression pattern of these five isoenzymes correlates with the relative role of anaerobic vs. aerobic metabolism of different tissues (29). Separation of the five LDH isoenzymes (Fig. 5A and B) in mtDNA mutator mice revealed an increase in those dominated by the *Ldh-A* product (M subunits) and a decrease of those rich in the *Ldh-B* product (H subunits), which, in turn, increase the P → L conversion. In 23-

wk-old mtDNA mutator mice, LDH-5 was increased 1.4-fold, and LDH-4 was increased 1.1-fold; however, LDH-1 was decreased 1.14-fold, and LDH-2 was decreased 1.09-fold. At 45 wk of age, these differences were enlarged. LDH-5 was increased twofold, and LDH-4 was increased 1.18-fold; however, LDH-1 was decreased 1.31-fold, and LDH-2 was decreased 1.14-fold. These observations are consistent with LDH-A and LDH-B gene expression pattern changes as determined by in situ hybridization, and reveal that LDH isoenzyme composition can shift as a reaction to mitochondrial dysfunction.

Functional Metabolic Shift to More Lactate Production. LDH activity may be measured from the pyruvate (P → L) or lactate (L → P) side of the reaction (30). A higher LDH_{P→L}/LDH_{L→P} ratio, known as the P:L ratio (31), signifies more LDH activity in the P → L direction (Fig. 5D). In 23-wk-old mtDNA mutator cortex, there was more P → L activity, and this activity increased as the mice aged. The percent change in LDH activity, measured from

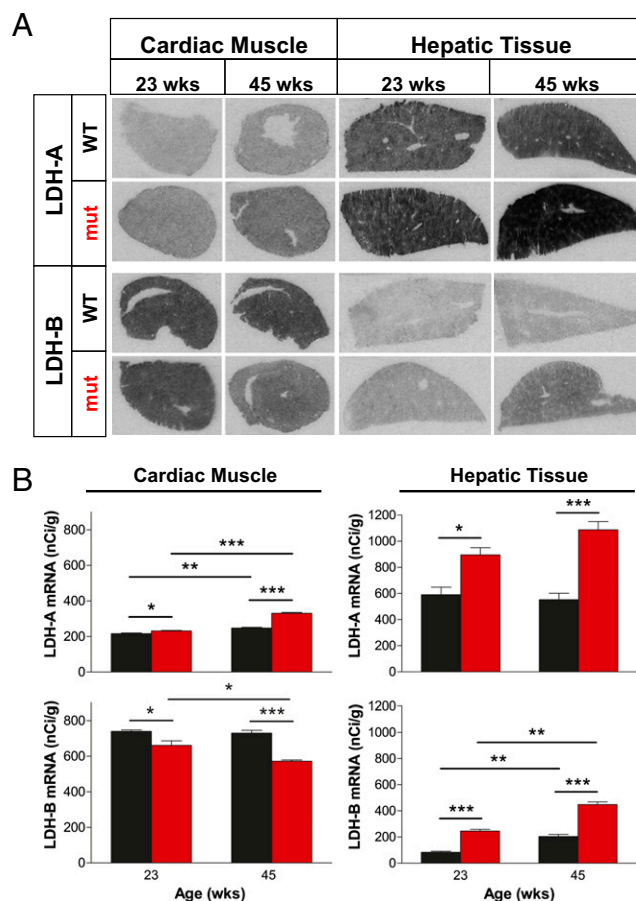
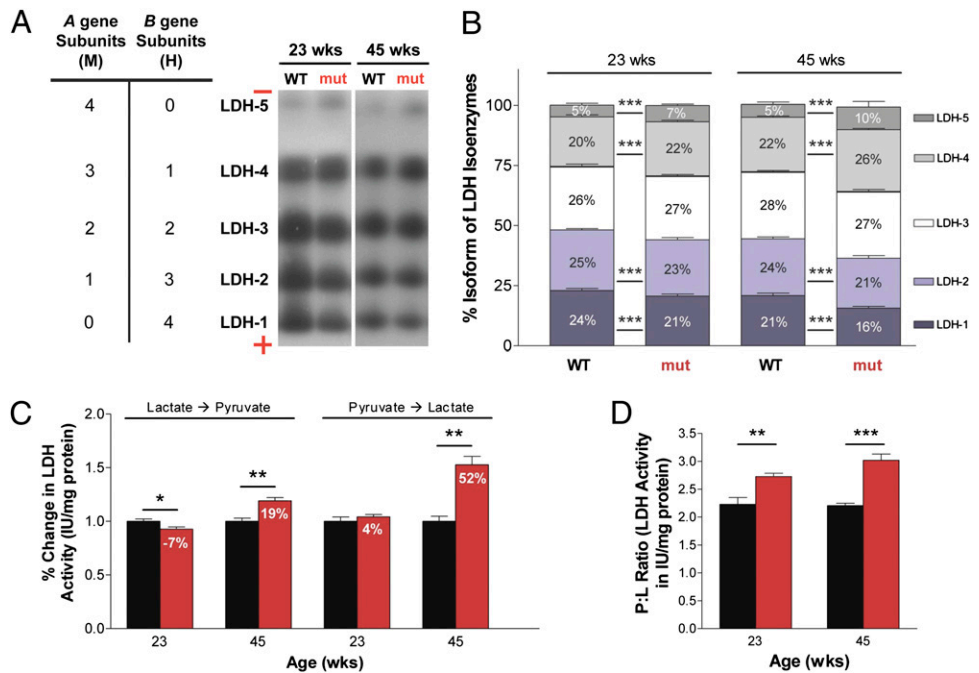


Fig. 4. Lactate dehydrogenase gene expression in peripheral tissues. (A) In situ hybridization of LDH-A and LDH-B mRNA in cardiac muscle and hepatic tissue sections from male 23-wk-old and 45-wk-old mtDNA mutator ($n = 6$; red) and age-matched littermate wild-type ($n = 6$; black) mice. (B) Quantification from autoradiographic films of LDH-A and LDH-B mRNA (mean values \pm SEM) expressed as nCi g⁻¹. In cardiac muscle, mtDNA mutator mice showed an up-regulation of LDH-A [$F(1,8) = 143$; $P < 0.0001$] and a down-regulation of LDH-B genes [$F(1,8) = 53.7$; $P < 0.0001$]. In both mtDNA mutator and wild-type mice, there was an increase in LDH-A mRNA levels as they aged [$t(4) = 15.1$; $P = 0.0001$ and $t(4) = 6.83$; $P = 0.002$, respectively], while LDH-B levels decreased with age only in mutator mice [$t(4) = 3.34$; $P = 0.029$]. In hepatic tissue, both LDH-A and LDH-B gene expression levels were up-regulated in mtDNA mutator mice [$F(1,8) = 55.1$; $P < 0.0001$ and $F(1,8)=186$; $P < 0.0001$, respectively]. Two-way between subjects ANOVA with posthoc analysis on age-matched groups (23 and 45 wk), and two-tailed unpaired t test to compare these groups. * $P < 0.05$, ** $P < 0.01$, and *** $P < 0.001$.

Fig. 5. A functional metabolic shift to more lactate production. Quantification of LDH isoenzymes and their collective enzymatic activity in cerebral cortex from 23- and 45-wk-old male mtDNA mutator ($n = 6$; red) and age-matched littermate wild-type ($n = 6$; black) mice. (A) LDH isoenzyme tetrameric composition (Left) indicates the number of M and H subunits that constitute each isoenzyme. Native gel electrophoresis of LDH isoenzymes (Right) showed the expression of all five isoenzymes in mtDNA mutator and wild-type cerebral cortex. The mobility of the isoenzymes was regulated by size and charge. (B) Quantification of LDH isoenzymes. In 23-wk-old mutator mice, there was increased expression (mean \pm SD) of isoenzymes comprised chiefly of M subunits [LDH-5: $t(28) = 7.69$; $P < 0.0001$ and LDH-4: $t(28) = 6.85$; $P < 0.0001$], which continued to increase with age [$t(28) = 6.31$; $P < 0.0001$ and $t(28) = 16.5$; $P < 0.0001$, respectively], and decreased expression in isoenzymes heavily composed of H subunits [LDH-1: $t(28) = 7.38$; $P < 0.0001$ and LDH-2: $t(28) = 6.33$; $P < 0.0001$], which continued to decrease with age [$t(28) = 8.14$; $P < 0.0001$ and $t(28) = 16.1$; $P < 0.0001$, respectively]. (C) Quantification of LDH activity determined from both the lactate and pyruvate sides of the reaction. Data, shown as percent change (mean \pm SEM) calculated from IU mg^{-1} protein, indicated a metabolic shift to more lactate production in mtDNA mutator mice, which increased with age from 11% to 33%. (D) The P:L ratio (mean \pm SEM) is a simplified reflection of the LDH activity (IU mg^{-1} protein) of all isoenzymes during interconversion of $\text{P} \leftrightarrow \text{L}$. The P:L ratio increased in 23-wk-old [$t(8) = 3.69$; $P = 0.006$] and 45-wk-old [$t(8) = 6.84$; $P = 0.0001$] mutator mice, showing higher LDH activity during $\text{P} \rightarrow \text{L}$ conversion. Analyses were performed by two-tailed unpaired t test to compare age-matched groups (23 and 45 wk). * $P < 0.05$, ** $P < 0.01$, and *** $P < 0.001$.



both the pyruvate and lactate sides of the reaction, shows a metabolic shift to lactate production in mtDNA mutator mice by 11% at 23 wk and 33% at 45 wk of age (Fig. 5C). These results, coupled with the LDH gene expression and isoenzymatic changes, show that the high lactate levels in both brain and peripheral tissues are the result of a metabolic shift to a glycolytic or anaerobic condition, where large amounts of lactate are being produced from pyruvate in an environment with increasingly dysfunctional mitochondria.

Discussion

Life Expectancy of mtDNA Mutator, "MILON," and MitoPark Neurons. The mtDNA mutator animals survive until ~46–48 wk of age, despite increasingly severe, chronic metabolic alterations. A similar phenomenon was previously seen in MILON mice (32), in which oxidative phosphorylation was shut down by removal of the mitochondrial transcription factor A (TFAM) in forebrain neurons. In these mice, respiratory chain-deficient telencephalic neurons survive for several months, suggesting that it is necessary for neurons to be exposed to a prolonged period of severe respiratory dysfunction before overt neurodegeneration begins. When dopamine neurons are instead deprived of TFAM, as in MitoPark mice (33), the animals survive approximately 1 y. In this case, TFAM removal occurs before birth, but the dopamine neurons show pathological changes during an extended period into and beyond the second month of life (34). Taken together, results from these transgenic mouse lines, all targeting mitochondrial function, suggest the presence of compensatory mechanisms that rely on anaerobic metabolism, the nature of which deserves further study.

Lactate as a Major Energy Source in the Brain. Cerebral lactate metabolism and its compartmentalization in astrocytes, neurons, and elsewhere is not fully understood (35). Lactate is continuously produced in brain, heart, skeletal muscle, and other tissues, even during completely aerobic conditions (36). It has been suggested that lactate constitutes an alternative source of energy

that the brain uses under strenuous situations (37). Furthermore, it has been shown that, under conditions of increased lactate production (i.e., exercise), the use of blood lactate as an energy source in the brain increases at the expense of blood glucose (38). Lactate is a substrate for the mitochondrial TCA cycle, and its oxidation can produce a significant amount of ATP (39). It is thought that an activity-regulated lactate shuttle from astrocytes to neurons would allow neurons to benefit from lactate (40). Although most recent modeling supports this theory (41–43) and lactate shuttling can be shown in brain slices (44), the neuron-glia metabolic interactions are not fully understood. The possibility of intracellular astrocyte and neuron lactate shuttles exists in addition to the potential for an astrocyte–neuron lactate shuttle (38). A recent microdialysis and high-resolution ^{13}C -NMR study showed that human brain cells can take up lactate from the extracellular space and process it through the TCA cycle (45). In the present study, we provide additional support for lactate as an energy substrate in the normal brain and find that the brain responds differently from heart and liver to decreasing oxidative phosphorylation. Thus, we argue that the brain's ability to produce and use lactate can be locally regulated by changing LDH-A/LDH-B gene activity ratios and controlling subunit composition of LDH isoenzymes, thereby allowing the brain to optimize use of energy resources and metabolism.

Lactate as a Noninvasive Symptomatic Marker of the Aging Process. In the present study, we establish that progressive failure of oxidative phosphorylation leads to metabolic alterations in both prematurely and normally aging mice. Reports indicate that cerebrospinal fluid lactate is elevated in aging humans (46–48). When healthy aging in humans was recently accessed with combined ^{13}C -/ ^1H -MRS, an association was found between reduced neuronal mitochondrial metabolism and altered glial mitochondrial metabolism in aged (76 ± 8 y) participants (49). Another study found that lactate levels measured by ^1H -NMR in 88- to 96-wk-old rats were significantly increased (50). In contrast, long-lived Ames dwarf mice have decreased plasma lactate levels (51). Our findings, coupled with recent research using ^1H -MRS and

biochemical assays to measure lactate and mitochondrial metabolism, support a role for lactate as a marker in aging, particularly in the brain. At present, there are few means to track symptomatic stages of CNS aging. Our data argue for the use of lactate $^1\text{H-MRS}$ as a noninvasive method to monitor this hallmark of the aging process. Comparing normally aging and mtDNA mutator mice allows us to conclude that the increased LDH-A/LDH-B gene expression ratio is causative of high brain lactate levels and that these lactate levels could predict aging. We have strong evidence that lactate levels are elevated in advance of other indices of aging in the prematurely aging mtDNA mutator mouse, and we have data to support that a similar pattern may characterize normal aging. The use of MRS will allow future studies to reveal when lactate levels begin to rise during the life of normal mice and how brain lactate levels may correlate to other indices of aging.

- Larsson NG (2010) Somatic mitochondrial DNA mutations in mammalian aging. *Annu Rev Biochem* 79:683–706.
- Harman D (1972) The biologic clock: The mitochondria? *J Am Geriatr Soc* 20:145–147.
- Wallace DC (1992) Mitochondrial genetics: A paradigm for aging and degenerative diseases? *Science* 256:628–632.
- Smeitink J, van den Heuvel L, DiMauro S (2001) The genetics and pathology of oxidative phosphorylation. *Nat Rev Genet* 2:342–352.
- Corral-Debrinski M, et al. (1992) Mitochondrial DNA deletions in human brain: Regional variability and increase with advanced age. *Nat Genet* 2:324–329.
- Soong NW, Hinton DR, Cortopassi G, Arnheim N (1992) Mosaicism for a specific somatic mitochondrial DNA mutation in adult human brain. *Nat Genet* 2: 318–323.
- Schwarze SR, et al. (1995) High levels of mitochondrial DNA deletions in skeletal muscle of old rhesus monkeys. *Mech Ageing Dev* 83:91–101.
- Khaidakov M, Heflich RH, Manjanatha MG, Myers MB, Aidoo A (2003) Accumulation of point mutations in mitochondrial DNA of aging mice. *Mutat Res* 526:1–7.
- Tanhauser SM, Laipis PJ (1995) Multiple deletions are detectable in mitochondrial DNA of aging mice. *J Biol Chem* 270:24769–24775.
- Cottrell DA, Turnbull DM (2000) Mitochondria and ageing. *Curr Opin Clin Nutr Metab Care* 3:473–478.
- Niu X, Trifunovic A, Larsson NG, Canlon B (2007) Somatic mtDNA mutations cause progressive hearing loss in the mouse. *Exp Cell Res* 313:3924–3934.
- Trifunovic A, et al. (2005) Somatic mtDNA mutations cause aging phenotypes without affecting reactive oxygen species production. *Proc Natl Acad Sci USA* 102:17993–17998.
- Trifunovic A, et al. (2004) Premature ageing in mice expressing defective mitochondrial DNA polymerase. *Nature* 429:417–423.
- Kujoth GC, et al. (2005) Mitochondrial DNA mutations, oxidative stress, and apoptosis in mammalian aging. *Science* 309:481–484.
- Edgar D, et al. (2009) Random point mutations with major effects on protein-coding genes are the driving force behind premature aging in mtDNA mutator mice. *Cell Metab* 10:131–138.
- Edgar D, Trifunovic A (2009) The mtDNA mutator mouse: Dissecting mitochondrial involvement in aging. *Aging (Albany NY)* 1:1028–1032.
- Vermulst M, et al. (2008) DNA deletions and clonal mutations drive premature aging in mitochondrial mutator mice. *Nat Genet* 40:392–394.
- Moore GJ, Galloway MP (2002) Magnetic resonance spectroscopy: Neurochemistry and treatment effects in affective disorders. *Psychopharmacol Bull* 36:5–23.
- Lin B, Busto R, Globus MY, Martinez E, Ginsberg MD (1995) Brain temperature modulations during global ischemia fail to influence extracellular lactate levels in rats. *Stroke* 26:1634–1638.
- Tkác I, et al. (2004) Highly resolved in vivo ^1H NMR spectroscopy of the mouse brain at 9.4 T. *Magn Reson Med* 52:478–484.
- Lin SS, Manchester JK, Gordon JI (2001) Enhanced gluconeogenesis and increased energy storage as hallmarks of aging in *Saccharomyces cerevisiae*. *J Biol Chem* 276: 36000–36007.
- Spindler SR (2001) Calorie restriction enhances the expression of key metabolic enzymes associated with protein renewal during aging. *Ann N Y Acad Sci* 928: 296–304.
- Cottrell DA, et al. (2001) Cytochrome c oxidase deficient cells accumulate in the hippocampus and choroid plexus with age. *Neurobiol Aging* 22:265–272.
- Gredilla R, Garm C, Holm R, Bohr VA, Stevnsner T (2010) Differential age-related changes in mitochondrial DNA repair activities in mouse brain regions. *Neurobiol Aging* 31:993–1002.
- Jazwinski SM (2005) The retrograde response links metabolism with stress responses, chromatin-dependent gene activation, and genome stability in yeast aging. *Gene* 354:22–27.
- Broadie RS, et al. (2004) Standardized quantitative in situ hybridization using radioactive oligonucleotide probes for detecting relative levels of mRNA transcripts verified by real-time PCR. *Brain Res* 1000:211–222.
- Laughton JD, et al. (2000) Differential messenger RNA distribution of lactate dehydrogenase LDH-1 and LDH-5 isoforms in the rat brain. *Neuroscience* 96:619–625.

Materials and Methods

For animal breeding and housing information, $^1\text{H-MRS}$ and metabolite determination/quantification, HPLC for lactate determination, tissue preparation for cryosectioning, enzyme histochemistry, in situ hybridization for LDH-A and LDH-B gene expression, microscopy, tissue preparation for enzymatic characterization, measurement of protein concentration, native gel electrophoresis for LDH isoenzyme characterization, spectrophotometric assays for LDH activity, and statistical analysis, see *SI Materials and Methods*.

ACKNOWLEDGMENTS. We thank Professor M. G. Masucci for support and the use of spectrophotometric equipment, E. Lindqvist and K. Lundströmer for technical assistance, and Dr. D. Marcellino for advice. This work was supported by the National Institute on Aging (AG04418), National Institute on Drug Abuse, National Institutes of Health—Karolinska Graduate Partnerships Program, Swedish Research Council, Swedish Brain Power, Swedish Brain Foundation, Karolinska Experimental Magnetic Resonance Center, and Karolinska Institutet Doctoral Funding.

- Miura S (1966) Lactic dehydrogenase isozymes of the brain. I. Electrophoretic studies on regional distribution and ontogenesis. *Folia Psychiatr Neurol Jpn* 20:337–347.
- Markert CL, Shaklee JB, Whitt GS (1975) Evolution of a gene. Multiple genes for LDH isozymes provide a model of the evolution of gene structure, function and regulation. *Science* 189:102–114.
- Amador E, Dorfman LE, Wacker WEC (1963) Serum lactic dehydrogenase activity: An analytical assessment of current assays. *Clin Chem* 12:391–399.
- Krieg AF, Rosenblum LJ, Henry JB (1967) Lactate dehydrogenase isoenzymes: a comparison of pyruvate-to-lactate and lactate-to-pyruvate assays. *Clin Chem* 13: 196–203.
- Sörensen L, et al. (2001) Late-onset corticohippocampal neurodepletion attributable to catastrophic failure of oxidative phosphorylation in MILON mice. *J Neurosci* 21:8082–8090.
- Ekstrand MI, et al. (2007) Progressive parkinsonism in mice with respiratory-chain-deficient dopamine neurons. *Proc Natl Acad Sci USA* 104:1325–1330.
- Galter D, et al. (2010) MitoPark mice mirror the slow progression of key symptoms and L-DOPA response in Parkinson's disease. *Genes Brain Behav* 9:173–181.
- Acosta ML, et al. (2005) Early markers of retinal degeneration in rd/rd mice. *Mol Vis* 11:717–728.
- Hashimoto T, Hussien R, Cho HS, Kaufer D, Brooks GA (2008) Evidence for the mitochondrial lactate oxidation complex in rat neurons: Demonstration of an essential component of brain lactate shuttles. *PLoS ONE* 3:e2915.
- Ekstrand F, Secher NH, Van Lieshout JJ (2008) Lactate fuels the human brain during exercise. *FASEB J* 22:3443–3449.
- van Hall G, et al. (2009) Blood lactate is an important energy source for the human brain. *J Cereb Blood Flow Metab* 29:1121–1129.
- Schurr A (2006) Lactate: The ultimate cerebral oxidative energy substrate? *J Cereb Blood Flow Metab* 26:142–152.
- Pellerin L, Magistretti PJ (1994) Glutamate uptake into astrocytes stimulates aerobic glycolysis: A mechanism coupling neuronal activity to glucose utilization. *Proc Natl Acad Sci USA* 91:10625–10629.
- Aubert A, Costalat R, Magistretti PJ, Pellerin L (2005) Brain lactate kinetics: Modeling evidence for neuronal lactate uptake upon activation. *Proc Natl Acad Sci USA* 102: 16448–16453.
- Aubert A, Pellerin L, Magistretti PJ, Costalat R (2007) A coherent neurobiological framework for functional neuroimaging provided by a model integrating compartmentalized energy metabolism. *Proc Natl Acad Sci USA* 104:4188–4193.
- Hyder F, et al. (2006) Neuronal-glia glucose oxidation and glutamatergic-GABAergic function. *J Cereb Blood Flow Metab* 26:865–877.
- Erlichman JS, et al. (2008) Inhibition of monocarboxylate transporter 2 in the retrotrapezoid nucleus in rats: A test of the astrocyte-neuron lactate-shuttle hypothesis. *J Neurosci* 28:4888–4896.
- Gallagher CN, et al. (2009) The human brain utilizes lactate via the tricarboxylic acid cycle: A ^{13}C -labelled microdialysis and high-resolution nuclear magnetic resonance study. *Brain* 132:2839–2849.
- Yesavage JA, Holman CA, Berger PA (1982) Cerebrospinal fluid lactate levels and aging: Findings in normals and patients with major depressive disorders. *Gerontology* 28:377–380.
- Yesavage JA, Holman CA, Sarnquist FH, Berger PA (1982) Elevation of cerebrospinal fluid lactate with aging in subjects with normal blood oxygen saturations. *J Gerontol* 37:313–315.
- Pryce JD, Gant PW, Sau KJ (1970) Normal concentrations of lactate, glucose, and protein in cerebrospinal fluid, and the diagnostic implications of abnormal concentrations. *Clin Chem* 16:562–565.
- Boumezbeur F, et al. (2010) Altered brain mitochondrial metabolism in healthy aging as assessed by in vivo magnetic resonance spectroscopy. *J Cereb Blood Flow Metab* 30: 211–221.
- Zhang X, et al. (2009) Metabonomic alterations in hippocampus, temporal and prefrontal cortex with age in rats. *Neurochem Int* 54:481–487.
- Romanick MA, Rakoczy SG, Brown-Borg HM (2004) Long-lived Ames dwarf mouse exhibits increased antioxidant defense in skeletal muscle. *Mech Ageing Dev* 125: 269–281.